

Vertically emitting, dye-doped polymer laser in the green ($\lambda \sim 536$ nm) with a second order distributed feedback grating fabricated by replica molding

M. Lu, B.T. Cunningham, S.-J. Park *, J.G. Eden

Department of Electrical and Computer Engineering, University of Illinois, Urbana, IL 61801, United States

Received 8 November 2007; received in revised form 26 January 2008; accepted 4 February 2008

Abstract

Lasing in the green from a distributed feedback (DFB) structure, based upon a second order grating fabricated by replica molding in a dye-doped UV curable polymer, has been demonstrated. For a Bragg grating having a periodicity and depth of 360 ± 2 nm and 78 ± 5 nm, respectively, a coumarin 540-polymer laser operates at 535.6 nm, which is in agreement with calculations of the photonic band diagram for the structure. The fabricated laser exhibits a linewidth of 0.15 nm, a threshold pump fluence of ~ 0.7 mJ cm⁻² at 355 nm, and a slope efficiency of $\sim 14\%$. Incorporation of the dye gain medium into a one- (or two-) dimensional photonic crystal and fabrication of the grating by replica molding at room temperature provides an inexpensive approach to fabricating polymer-based DFB lasers on flexible substrates of large area.

© 2008 Elsevier B.V. All rights reserved.

1. Introduction

Since the demonstrations (in 1971) of lasing in which optical feedback was realized by a corrugated, periodic refractive index structure [1,2], organic dyes have offered a versatile gain medium for the evaluation of integrated resonator designs, waveguide configurations and microlaser fabrication techniques [3–12]. Suitable for incorporation into polymers, sol-gel silica [6], and other hosts such as zirconia [7], dyes have conveniently provided the requisite gain for the development of optical resonators based on distributed feedback (DFB) [6–12], distributed Bragg reflectors (DBRs) [4] or microdisks [3]. DFB structures offer periodic modulation of either the gain [6–9] or refractive index [10–12] of the medium and are generally preferred for solid state dye lasers, principally because end-on or out-of-plane emission, broad tunability, and narrow linewidth [8] are available. A drawback of conventional

refractive index-modulated DFB dye laser designs, however, is the requirement for electron beam lithography [10] or interference photolithographic techniques [11,12] to define the one- or two-dimensional surface grating.

Recently introduced embossing and imprinting techniques have simplified grating fabrication with inexpensive processes amenable to high throughput manufacturing and yet capable of precisely reproducing submicron features in a polymer substrate. Although embossing methods have reproduced submicron periodic grating patterns, the elevated pressures and temperatures required result in the accumulation of defects in the embossing tool and render the process incompatible with plastic film substrates (such as polyester and polycarbonate). It should also be noted that Ichikawa et al. [13] recently described a DFB laser fabricated by thermally-cured replica molding but the linewidth was measured to be 0.6 nm.

Ultraviolet (UV)-cured nanoreplica molding is, in contrast, a room temperature, low pressure process for the transfer of surface structure from a silicon wafer onto a flexible plastic substrate. Features with depths and widths as small as 10 nm, and one- and two-dimensional gratings

* Corresponding author. Tel.: +1 2174938477; fax: +1 2172447097.
E-mail address: sjinpark@uiuc.edu (S.-J. Park).

with periods as low as 230 nm, have been reported [14]. Photonic crystal optical filters and biosensors fabricated by nanoreplica molding are currently manufactured by a large area, continuous roll-to-roll process [15].

This Letter reports the demonstration and characterization of lasing in the green ($\lambda \sim 536$ nm) from a polymer-based DFB laser in which the dye gain medium is incorporated into a high-index, second order DFB grating. Fabricated by nanoreplica molding and optically pumped at 355 nm and an arbitrary angle of incidence, this integrated laser exhibits a threshold pump fluence of ~ 0.7 mJ cm⁻² for coumarin 540 dye, a slope efficiency of $\sim 14\%$, and a lifetime (to half power) of ~ 800 shots.

2. Device structure and fabrication

A cross-sectional diagram (not to scale) of the DFB laser structure adopted for the present experiments is shown in Fig. 1. A polymer cladding layer was first applied to one surface of a polyethylene-terephthalate (PET) substrate by replica molding. A liquid, ultraviolet (UV)-curable polymer (Luvantix WR-354) with a refractive index of 1.39 was squeezed between the PET substrate and a planar, 10 cm (4 in.) dia. Si wafer having no surface structure. In order to ensure the thickness uniformity of the resulting polymer film, this room temperature molding process occurred while compressing the Si and liquid polymer with a 2.3 kg (5 lb) roller to yield a 10 μ m thick layer. Illumination of the polymer film through the PET substrate with UV radiation for 30 s solidified the cladding by photopolymerization. After separating the Si wafer and cladding replica, the surface of the cladding was exposed to an O₂ plasma for 5 min in order to improve adhesion between the cladding and active layers. The latter was fabricated by preparing a 40 mg/mL solution of coumarin 540 dye and CH₂Cl₂, and mixing the solution with a polymer (NOA88, Norland Products) to a volume percentage of 10%. This material was sonicated for improved homogenization, and subsequently heated in a 40 °C water bath for 20 min. to evaporate the CH₂Cl₂ solvent and decrease the polymer viscosity. The dye/polymer solution was then spin-coated onto the cladding-substrate assembly at 7000 rpm. Fabrication of the DFB grating profile in the surface of the active layer was again accomplished by rep-

lica molding with a second Si wafer onto which the desired grating pattern had been produced by conventional deep UV lithography, reactive ion etching to a depth of ~ 80 nm, and removal of the photoresist. The completed DFB active layer has an overall thickness of ~ 500 nm as measured by a surface profilometer.

3. Grating characteristics

In addition to the integration of the gain medium into the DFB structure, a key aspect of the laser design of Fig. 1 is the incorporation of a second order grating. Unlike first order DFB structures, second order gratings support both edge and surface (out-of-plane) emission modes. Specifically, the second order DFB grating couples laser radiation into a vertically-emitted mode by first order diffraction [16]. Furthermore, maximum reflectivity for this one-dimensional photonic crystal occurs at the resonance wavelength which corresponds to the lower band edge of the structure [17]. For the 360 nm period DFB cavity of Fig. 1, the resonance wavelength was calculated by rigorous coupled-wave analysis (RCWA) for wavelengths in the 450–600 nm interval (spectral extent of coumarin 540 dye operation) and $0^\circ \leq \theta_r \leq 8^\circ$, where θ_r is the angle of the emitted (DFB laser) radiation with respect to the normal of the surface grating. If ten spatial harmonics are included in one period of the grating structure, the result is illustrated in Fig. 2. It is evident from the diagram that, in the direction $\theta_r = 0$, the resonant wavelength of the DFB structure is ~ 535.4 nm. A surface profile of the grating, recorded with an atomic force microscope (AFM), and a scanning electron micrograph (SEM) of the DFB structure are presented in Fig. 3. Both verify that the periodicity and depth of the grating are 360 ± 2 nm and 78 ± 5 nm, respectively. Replicated grating resonators with active areas as large as 1×1 cm² have been fabricated and tested to date.

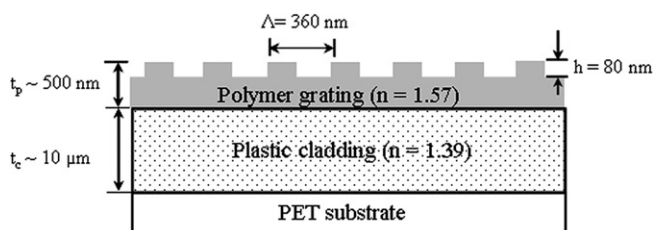


Fig. 1. Cross-sectional diagram (not to scale) of the polymer DFB laser structure. Both the cladding and active (dye/polymer) layers were fabricated in UV-curable polymers by replica molding.

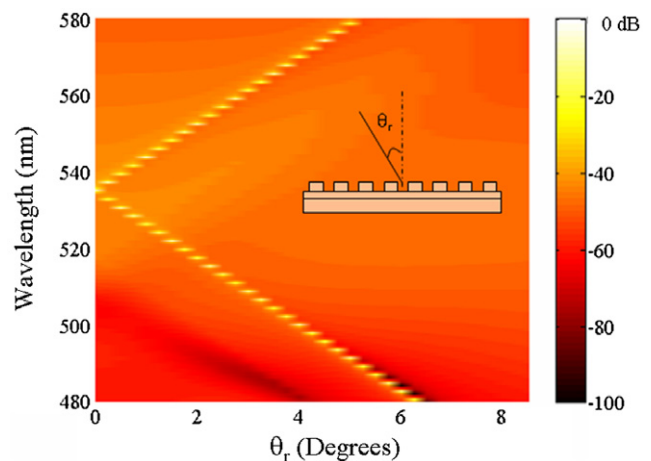


Fig. 2. Photonic band diagram for the structure of Fig. 1, calculated for $0^\circ \leq \theta_r \leq 8^\circ$ where θ_r is the angle of the DFB laser radiation with respect to the normal of the surface grating.

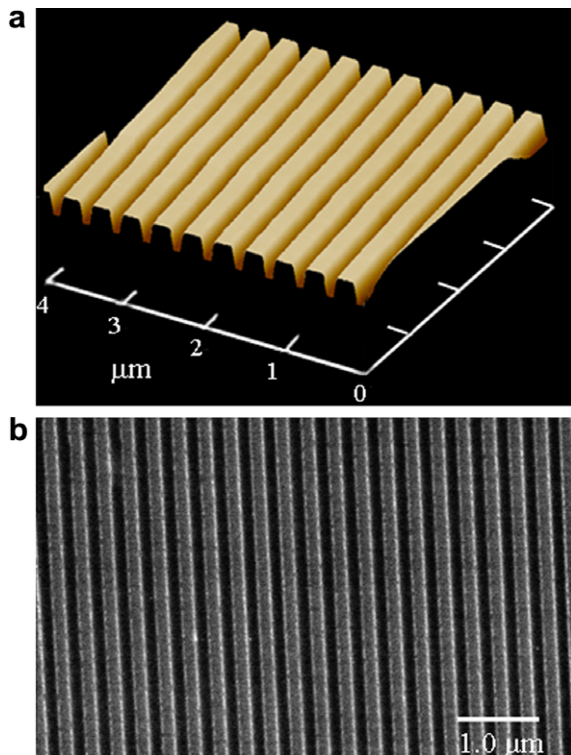


Fig. 3. (a) AFM profile and (b) SEM image of the replicated DFB grating. The period and depth of the structure are 360 ± 2 nm and 78 ± 5 nm, respectively.

4. Experimental results and discussion

Optical pumping experiments were conducted by exciting the coumarin 540, DFB structure with ≤ 10 ns FWHM pulses from a frequency-tripled, Q-switched Nd:YAG laser. Pump fluence at the sample was varied with neutral density filters and emission emanating from the grating was monitored along the axis orthogonal to the surface with a spectrometer (Ocean Optics HR4000) having a resolution (in first order) of 0.12 nm FWHM. Spectra representative of those recorded for pump fluences of 0.5 mJ cm^{-2} and 1.5 mJ cm^{-2} are shown in Fig. 4. For a fluence below threshold (0.5 mJ cm^{-2}), the fluorescence from the dye/polymer matrix is broad (~ 62 nm FWHM) and the spectral profile is slightly skewed to the red. At higher intensities, laser oscillation occurs at 535.6 nm which is in excellent agreement with the calculated value (535.4 nm) and yet is slightly offset from the wavelength at which peak spontaneous emission occurs. Owing to the small modulation of the refractive index afforded by the polymer grating structure of Fig. 1, the photonic bandgap vanishes for wave vectors normal to the grating surface, resulting in lasing at a single wavelength (as opposed to the dual mode operation of Ref. [18]) and radiation emerging from the device at $\theta_r = 0$ [5–7,10–12]. Although instrument-limited, the measurement of the laser linewidth yields ~ 0.15 nm which is one-quarter of the value reported [13] for a DFB laser having a thermally-cured, replica-molded grating. The transverse profile of the radiation emerging

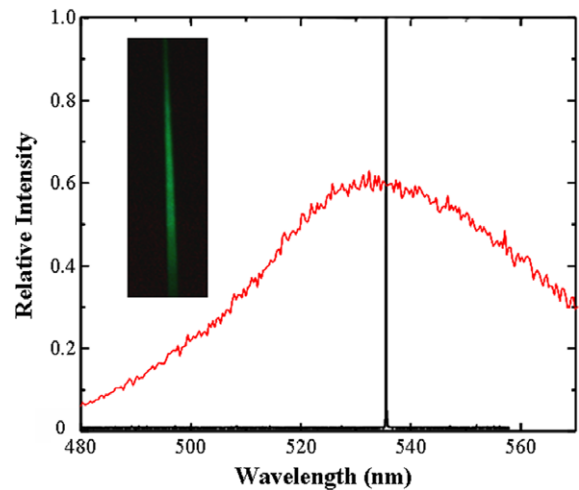


Fig. 4. Spontaneous emission and laser spectra for the coumarin 540/polymer DFB structure, recorded for 355 nm pump energy fluences of 0.5 mJ cm^{-2} and 1.5 mJ cm^{-2} , respectively. The inset is a photograph (recorded by a CCD camera) of the beam emerging from the DFB laser.

from the laser, illustrated by the inset to Fig. 4, was recorded with a CCD camera. Because a one-dimensional DFB resonator provides optical confinement only in the direction perpendicular to the grating axis, the beam divergence along the coordinate parallel to the axis of the grating is large ($>2^\circ$) [19].

Fig. 5 summarizes measurements, with a pyroelectric detector, of the dependence of the DFB laser pulse energy on the pump fluence (Φ). A clear threshold fluence of $\sim 0.7 \text{ mJ cm}^{-2}$ is observed and at higher intensities the output rises linearly with pump power as exhibited by the linear least-squares fit to the $\Phi \geq 0.7 \text{ mJ cm}^{-2}$ data. Note that the slope efficiency for this DFB laser is 14%. Preliminary lifetime data for the DFB laser structure reported here have also been obtained with a pump fluence of

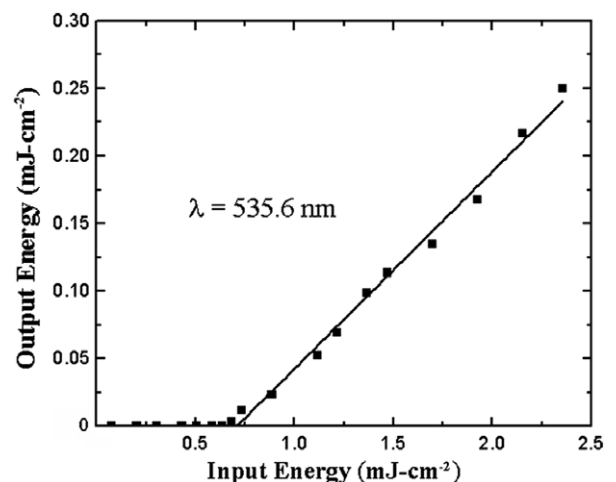


Fig. 5. Dependence of the relative, peak laser output power on the pump fluence for an excitation wavelength of 355 nm. Threshold lies at $\sim 0.7 \text{ mJ/cm}^2$ and the solid line (having a slope of $\sim 14\%$) is the least-squares fit to the above-threshold data.

1.0 mJ cm⁻² and a pulse repetition frequency of 1 Hz. After decreasing by 50% in the first ~800 pulses, the relative peak intensity of the laser continues to decline (but more slowly) and reaches 10% of its initial value after ~1600 pulses. Because no damage to the DFB grating or polymer/dye film is noticeable after 10⁴ pulses, one concludes that degradation of the laser output intensity arises from bleaching of the organic dye. We also note that the device lifetimes observed to date are consistent with otherwise identical laser structures having a PMMA polymer host.

5. Conclusions

In summary, lasing in the green from a polymer-based DFB laser, having dye incorporated into a second order grating, has been demonstrated and characterized. Exhibiting a threshold pump fluence of ~0.7 mJ cm⁻² and fabricated by a room temperature replica-molding process, this DFB polymer-dye structure is inexpensive and manufacturable on plastic substrates of large surface area. These devices offer the opportunity to pursue coupled cavity configurations and phased arrays in a compact planar technology.

Acknowledgements

This work was supported by SRU Biosystems and the National Science Foundation under Grant No. 0427657. Any opinions, findings, and conclusions or recommendations expressed in this article are those of the authors and do not necessarily reflect the views of the National Science Foundation. The technical assistance of C.J. Wagner and

B.J. Ricconi of the Laboratory for Optical Physics and Engineering is gratefully acknowledged.

References

- [1] H. Kogelnik, C.V. Shank, *Appl. Phys. Lett.* 18 (1971) 152.
- [2] I.P. Kaminov, H.P. Weber, E.A. Chandross, *Appl. Phys. Lett.* 18 (1971) 497.
- [3] M. Kuwata-Gonokami, R.H. Jordan, A. Dodabalapur, H.E. Katz, M.L. Schilling, R.E. Slusher, S. Ozawa, *Opt. Lett.* 20 (1995) 2093.
- [4] M. Berggren, A. Dodabalapur, R.E. Slusher, *Appl. Phys. Lett.* 71 (1997) 2230.
- [5] J.A. Rogers, M. Meier, A. Dodabalapur, E.J. Laskowski, M.A. Cappuzzo, *Appl. Phys. Lett.* 74 (1999) 3257.
- [6] X. Zhu, S. Lam, D. Lo, *Appl. Opt.* 39 (2000) 3104.
- [7] C. Ye, J. Wang, L. Shi, D. Lo, *Appl. Phys. B* 78 (2004) 189.
- [8] V.M. Katarkevich, A.N. Rubinov, S.A. Ryzhechkin, T.Sh. Efendiev, *Quantum Electron.* 24 (1994) 871.
- [9] W.J. Wadsworth, I.T. McKinnie, A.D. Woolhouse, T.G. Haskell, *Appl. Phys. B* 69 (1999) 163.
- [10] S. Balslev, T. Rasmussen, P. Shi, A. Kristensen, *J. Micromech. Microeng.* 15 (2005) 2456.
- [11] N. Nakai, M. Fukuda, K. Mito, *Jpn. J. Appl. Phys.* 45 (2006) 998.
- [12] Y. Oki, K. Aso, D. Zuo, N.J. Vasa, M. Maeda, *Jpn. J. Appl. Phys.* 41 (2002) 6370.
- [13] M. Ichikawa, Y. Tanaka, N. Suganuma, T. Koyama, Y. Taniguchi, *Jpn. J. Appl. Phys.* 42 (2003) 5590.
- [14] N. Ganesh, B.T. Cunningham, *Appl. Phys. Lett.* 88 (2006) 071110.
- [15] B. Cunningham, B. Lin, J. Qiu, P. Li, J. Pepper, B. Hugh, *Sens. Actuators, B* 85 (2002) 219.
- [16] C.H. Henry, R.F. Kazarinov, R.A. Logan, R. Yen, *IEEE J. Quantum Electron.* QE-21 (1985) 151.
- [17] Y. Ding, R. Magnusson, *Opt. Express* 15 (2007) 680.
- [18] S.L. McCall, P.M. Platzman, *IEEE J. Quantum Electron.* QE-21 (1985) 1899.
- [19] G. Heliotis, R. Xia, G.A. Turnbull, P. Andrew, W.L. Barnes, I.D.W. Samuel, D.D.C. Bradley, *Adv. Funct. Mater.* 14 (2004) 91.